Phase-Shifted Carrier-Based Synchronized Sinusoidal PWM Techniques for a Cascaded H-Bridge Multilevel Inverter

Saroj Kumar Sahoo, *Student Member, IEEE*, and Tanmoy Bhattacharya, *Member, IEEE*

***Abstract*—This paper analyzes synchronization strategy for cascaded H-bridge multilevel inverter (CHBMLI) topologies with a carrier-based sinusoidal phase-shifted pulse width modulation (PSPWM) technique. In the PSPWM technique, a separate carrier is used for each H-bridge (HB). The carriers are generally phase shifted from each other by π/x rad (x = No. of HBs) for unipolar PWM. With the carrier frequency being an integer (odd/even) multiple of the fundamental frequency, it is observed that the positions of zero crossings of the carriers with respect to the zero crossings of voltage references play an important role for maintaining quarter-wave symmetry among multilevel inverter pole voltage waveforms. This paper analytically shows the conditions for half-wave symmetry and quarter-wave symmetry and experimentally verifies those conditions for the PSPWM technique with a five-level CHBMLI laboratory prototype.**

***Index Terms*—Cascaded H-bridge multilevel inverter (CHBMLI), half-wave symmetry (HWS), phase-shifted carrier-based pulse width modulation (PWM), quarter-wave symmetry (QWS), synchronous PWM.**

I. Introduction

With the increasing demand of medium voltage and high power drives, the use of multilevel inverters (MLIs) is gradually becoming more and more important. This is due to reduced voltage stress on semiconductor devices, reduced harmonics in inverter output voltage, and lesser electromagnetic interferences. For medium voltage and high power applications, the switching frequency and device ratings are limited [1]–[3]. Increasing the power rating by minimizing the switching frequency while still maintaining reasonable power quality is an important requirement and a persistent challenge [2], [3]. Hence, the use of MLIs suitably distributes the stress among the semiconductor switches. Among the different MLI topologies, the cascaded H-bridge (CHB) topology is a preferred choice for medium voltage drives for its modularity and this is also the target converter for the proposed pulse width modulation (PWM) technique in this paper.

Manuscript received August 30, 2016; revised November 2, 2016; accepted January 31, 2017. Date of publication February 14, 2017; date of current version October 6, 2017. This work was supported by the Science and Energy Research Board, Department of Science and Technology (India) through project no. SB/S3/EECE/0188/2013. Recommended for publication by Associate Editor Alireza Nami.

The authors are with the Department of Electrical Engineering, Indian Institute of technology, Kharagpur, Kharagpur 721302, India (e-mail: sarojsahoo.mdpe@gmail.com; btanmoy@ee.iitkgp.ernet.in).

Color versions of one or more of the figures in this paper are available online at http://ieeexplore.ieee.org.

Digital Object Identifier 10.1109/TPEL.2017.2669084

In high power and medium voltage applications, the power converters operate at low switching frequency. This is very well defined in the literature as low pulse ratio operation of the converters. The applications consist of traction drives (both voltage source inverter (VSI)- and current source inverter (CSI)-fed drives), grid applications (as bidirectional converters, active power filters), etc. As the pulse ratio is less in these power converters, lower order harmonics including subharmonics are introduced in line currents resulting in higher total harmonic distortion (THD). Hence, synchronization among PWM voltages is necessary. Along with synchronization, the PWM voltage should maintain half-wave, quarter-wave, and three-phase symmetries [4], [5]. Narayanan [6] shows the advantages of maintaining the above-mentioned waveform symmetries. The synchronization ensures the PWM voltage is free from the subharmonics. Three-phase symmetry among the PWM voltages ensures the fundamental and the harmonics are balanced and also free from dc offset. Moreover, three-phase symmetry also ensures that the triplen harmonics are in phase and appear as zero sequence voltage with the advantage of not contributing to the ripple current. Half-wave symmetry ensures the PWM voltages are free from even-order harmonics. Although quarter-wave symmetry does not eliminate any harmonics, it ensures that the existing fundamental and harmonics have only sine component and eliminates the possibility of phase error between the reference and the fundamental output voltage. Buja and Indri [7] propose an optimal PWM scheme for two-level inverters to reduce current harmonics with offline calculations of switching pattern. This optimized PWM strategy can also be extended to MLIs. Edpuganti and Rathore [8] show the application of the synchronized optimal PWM technique for a cascaded nine-level inverter, where the average device switching frequency is limited to rated fundamental frequency. Rathore *et al*. [9] compare the performances of five-level and seven-level neutral point clamped (NPC) inverters with the synchronous optimal PWM technique. But, the synchronized optimal PWM technique is an offline calculation based technique. The switching angles are precalculated assuming steady-state condition and this requires storage of large data for better accuracy. Holtz and Oikonomou [10] propose a trajectory tracking control for three-level NPC with the synchronous optimal PWM technique. Geyer *et al*. [11] propose the model predictive pulse pattern control for a five-level NPC inverter with the optimized PWM technique.

Selective harmonic elimination and selective harmonic mitigation PWM techniques are the other alternatives. Haw *et al.* [12] show the application of the selective harmonic elimination PWM (SHEPWM) technique for cascade MLIs, whereas [13] shows the use of the selective harmonic mitigation PWM (SHMPWM) technique. But they are also the offline calculation based PWM technique and require lookup tables for implementation, hence the more microcontroller memory space. Zhang *et al.* [14]–[16] show the application of the online harmonic compensation scheme to improve the existing SHEPWM technique for high-power converters. These references mainly focus on grid-connected high-power converters (i.e., current source rectifiers).

All the above-mentioned MLI PWM techniques (synchronous optimal PWM (SOPWM), SHEPWM, and selective harmonic mitigation PWM (SHMPWM) techniques, leaving online harmonic compensation scheme) are based on offline calculations. The calculation complexity increases with increase in the number of voltage levels or increase in the number of commutation angles at lower modulation indexes. But the carrier-based PWM techniques are independent of motor parameters, independent of optimization, and do not require offline calculation or look-up tables to generate firing angles. Hence, the carrier-based PWM technique is well-suited to MLIs although the harmonic contents of the inverter output pole voltage are not optimized. Two carrier-based PWM techniques are available in the literature for MLIs. They are 1) level-shifted PWM (LSPWM) technique and 2) phase-shifted PWM (PSPWM) technique. But, the major challenge for the carrier-based PWM techniques for MLIs is to position the zero crossings of carriers' with respect to the zero crossings of voltage references so that different symmetries among pole voltage waveforms can be maintained. For two-level inverters, synchronization with different symmetries is achievable if the zero crossings of the carrier matches with the zero crossings of the voltage references and the ratio "*p*" ($p = f_c/f_s$ where $f_c =$ carrier frequency and $f_s =$ voltage reference frequency) is maintained to be an odd integer (multiple of 3). The carrier synchronization with the voltage references is sufficient for the LSPWM technique for CHBMLIs, as only one synchronous carrier is sufficient to implement different voltage levels [17]. Hence, the pole voltage maintains all the basic properties of an ideal synchronous PWM technique. But, the power distribution and average device switching frequencies of different H-bridges (HBs) are different.

But this scenario is completely different for the PSPWM technique, as multiple phase-shifted synchronous carriers are used for different HBs. So, it is impossible to match the zero crossings of each carrier with the voltage reference zero crossings. Hence, the positions of the zero crossings of voltage references with respect to the zero crossings of carriers play an important role for maintaining different basic properties of an ideal synchronous PWM, as stated in the previous paragraph. This paper mainly deals with the analytical studies for maintaining half-wave symmetry and quarter-wave symmetry among CHBMLI pole voltage waveform with the synchronous sinusoidal PSPWM technique. The carriers used for the analysis in this paper are generated from the instantaneous voltage references, as in [17]–[19] and always maintain an integer ratio *p*.

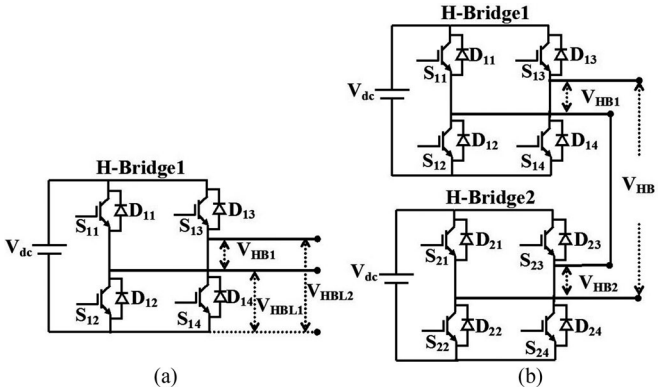

Fig. 1. (a) Single H-bridge and (b) double-cascaded H-bridges.

This paper is arranged as follows. Section II deals with the analytical explanation for the PSPWM technique to maintain synchronization, three-phase symmetry, half-wave symmetry, and quarter-wave symmetry among CHBMLI pole voltage waveforms. Experimental results are given in Section III and the paper is concluded in Section IV.

II. Conditions of Phase-Shifted Synchronous PWM for CHBMLI

The unipolar PWM technique is used for generating gate pulses for each HB. The HB pole voltage varies between 0 and $+V_{\rm dc}$ when the sign of the voltage reference is positive and varies between 0 and $-V_{\rm dc}$ when the sign of the voltage reference is negative (where $V_{\rm dc}$ is the input dc link voltage of the HB). For implementing unipolar PWM in an HB1 [see Fig. 1(a)], a positive voltage reference R_1 is used to generate gate pulses for switches S_{11} and S_{12} of leg1 and a negative voltage reference R_2 is used to generate gate pulses for switches S_{13} and S_{14} of leg2. A common carrier $C_{\rm HB1}$ is used for both the legs in order to generate gate pulses. The resultant output pole voltage $V_{\rm HB1}$ is the algebraic summation of individual leg voltages, i.e., $V_{\rm HB1} = V_{\rm HBL1} - V_{\rm HBL2}$.

A. Verification of Synchronization

The synchronization between voltage reference and fundamental component of inverter output pole voltage can be maintained if the synchronous carrier frequency is *n* (*n* being any integer) times the voltage reference frequency. By maintaining the above-mentioned condition, the intersection points between the carrier and the voltage reference (i.e., in a fundamental cycle of the voltage reference) repeat after 2π rad (i.e., the next consecutive fundamental cycle of the voltage reference), hence synchronization is maintained.

B. Verification of Three-Phase Symmetry and Half-Wave Symmetry

With synchronous carriers having $3n$ times the fundamental frequency (*n* being any integer) being used for the PSPWM technique, three-phase symmetry is always maintained among individual HB output pole voltage waveforms. Also, from Fig. 2(a)

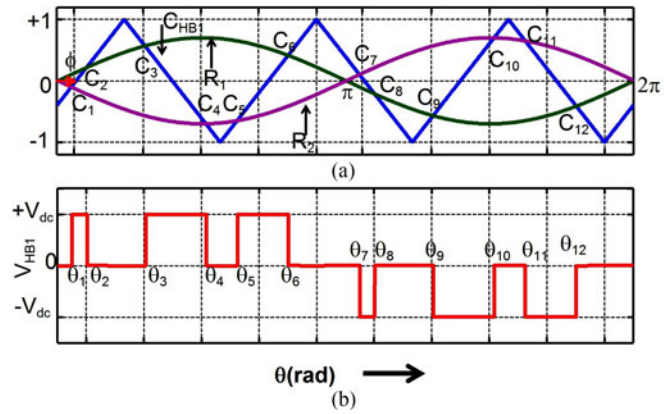

Fig. 2. (a) Carrier C_{HB1} lagging the normalized voltage references R_1 and R_2 by Φ rad ($f_c/f_s = 3$) and (b) pole voltage V_{HB1}.

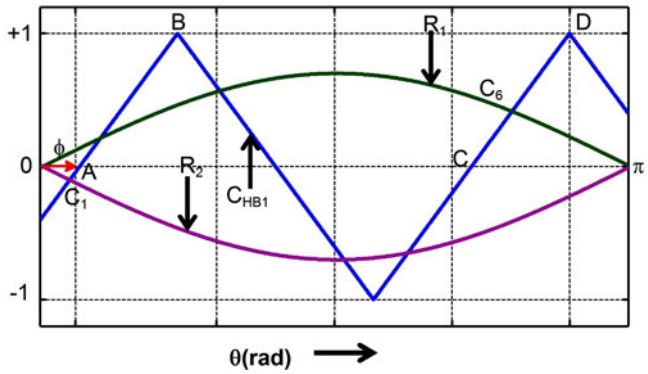

Fig. 3. Carrier C_{HB1} lagging the normalized voltage references R_1 and R_2 by Φ rad ($f_c/f_s = 3$).

it can be observed that for an odd integer ratio between the carrier and fundamental frequency, the region from π to 2π rad is equivalent to a mirror image of the region from 0 to π rad with respect to x-axis (θ). Hence, the intersection points C_1–C_6 are the mirror images of points from C_7 to C_{12}, respectively. In fact, for an odd integer ratio, individual pole voltages of both the legs (V_{HBL1} and V_{HBL2}) of one HB maintain half-wave symmetry and hence their difference also maintains half-wave symmetry. If the ratio is even then, individual pole voltages of both the legs (V_{HBL1} and V_{HBL2}) do not maintain half-wave symmetry. But the waveform of V_{HBL1} from 0 to π rad is an exact replica of V_{HBL2} from π to 2π rad and vice versa. Hence, their difference (i.e., $V_{\mathrm{HB1}} = V_{\mathrm{HBL1}} - V_{\mathrm{HBL2}}$) maintains half-wave symmetry. Hence, for an HB, the half-wave symmetry is satisfied for any carrier having its frequency equal to integer (odd/even) multiple of the fundamental frequency. Therefore, it can be concluded that the inverter pole voltage waveform maintains three-phase and half-wave symmetry for carriers having $3n$ times the fundamental frequency (n being any odd/even integer). It is, therefore, only necessary to determine the conditions for quarter-wave symmetry in the inverter output pole voltage waveform.

C. Determination of Conditions for Quarter-Wave Symmetry

1) Single H-Bridge: The quarter-wave symmetry among pole voltage waveform of an HB [see Fig. 1(a)] can be maintained, if the positive zero crossing of the voltage reference coincides with the positive zero crossing of the carrier. The normalized fundamental voltage references are sine waves with their amplitude less than or equal to one. The carriers are triangular waves with the magnitude of their positive and negative peaks equal to one. Positive zero crossing means the instantaneous values of these periodic waveforms have completed their negative half-cycles and become zero before entering the positive half-cycle. The carrier can be of two types. They are 1) in-phase carrier (positive zero crossing of positive voltage reference coincides with the positive zero crossing of the carrier) and 2) out-of-phase carrier (positive zero crossing of the positive voltage reference coincides with the negative zero crossing of the carrier). For carrier frequency being an odd multiple of the fundamental frequency, individual pole voltages of both the legs (V_{HBL1} and V_{HBL2}) maintain quarter-wave symmetry ensuring quarter-wave symmetry of the bridge output voltage V_{HB1}. For carrier frequency being an even multiple of the fundamental frequency, individual pole voltages of both the legs (V_{HBL1} and V_{HBL2}) do not maintain quarter-wave symmetry. But their difference $V_{\mathrm{HB1}} = V_{\mathrm{HBL1}} - V_{\mathrm{HBL2}}$ maintains quarter-wave symmetry.

If the carrier is phase delayed by $\pi/2$ rad (where 2π rad is one carrier period), then the reverse phenomenon occurs. Now, for carrier frequency being an even multiple of the fundamental frequency, individual pole voltages of both the legs (V_{HBL1} and V_{HBL2}) maintain quarter-wave symmetry. Whereas for carrier frequency being an odd multiple of the fundamental frequency, individual pole voltages of both the legs (V_{HBL1} and V_{HBL2}) do not maintain quarter-wave symmetry. But their difference $V_{\mathrm{HB1}} = V_{\mathrm{HBL1}} - V_{\mathrm{HBL2}}$ maintains quarter-wave symmetry. This can also be derived mathematically as shown in the following discussion. As a specific case, the carrier frequency is taken to be three times the fundamental frequency.

From Fig. 2, for maintaining quarter-wave symmetry of the pole voltage waveform V_{HB1}, the constraint to be satisfied among voltage reference and carrier intersection points C_1–C_6 is given by

$$\theta_{7-l} = \pi - \theta_l \quad \text{for } l = 1,\ 2,\ \text{and } 3. \tag{1}$$

For $l = 1$, the values of θ_1 and θ_6 at points C_1 and C_6 can be found out by equating the equations of voltage reference's and the carrier's. A small step is shown below to determine the equations of voltage references and carriers at points C_1 and C_6 with the help of (2)–(5). Fig. 3 shows the enlarged view of voltage references R_1 and R_2 along with carrier C_{HB1}. The point C_1 [whose trace is θ_1 along x-axis (θ)] is the intersection point between voltage reference R_2 and line AB which is one part of the carrier C_{HB1}.

The equation of the voltage reference at C_1 can be written as

$$z_1 = -m \sin \theta_1. \tag{2}$$

The co-ordinates of the points A and B are (Φ, 0) and ($\Phi + \pi/6,\ 1$), respectively. Hence, the equation of the line AB at point

C_1 can be written as

$$z_1 = \left(\frac{6}{\pi}\right)(\theta_1 - \phi). \tag{3}$$

Similarly, the point C_6 is the intersection point between R_1 and line CD (which is a portion of carrier C_{HB1}).

The equation of the voltage reference at C_6 can be written as

$$z_6 = m \sin \theta_6. \tag{4}$$

The co-ordinates of the points C and D are $(2\pi/3 + \Phi,\ 0)$ and $(\Phi + 5\pi/6,\ 1)$, respectively. Hence, the equation of the line CD at point C_6 can be written as

$$z_6 = \left(\frac{6}{\pi}\right)\left(\theta_6 - \frac{2\pi}{3} - \phi\right) \tag{5}$$

where z_1 and z_6 = y-axis values at points C_1 and C_6, respectively, and m = modulation index of voltage references R_1 and R_2.

From (2) to (5), the intersection angles θ_1 and θ_6 at points C_1 and C_6 can be found out by equating the equations of voltage references and carriers and can be written, respectively, as

$$-m \sin \theta_1 = \left(\frac{6}{\pi}\right)(\theta_1 - \phi) \tag{6}$$

$$m \sin \theta_6 = \left(\frac{6}{\pi}\right)\left(\theta_6 - \frac{2\pi}{3} - \phi\right). \tag{7}$$

By putting the constraint of quarter-wave symmetry (2), (7) can be modified as

$$m \sin \theta_1 = \left(\frac{6}{\pi}\right)\left(\frac{\pi}{3} - \theta_1 - \phi\right). \tag{8}$$

By adding (6) and (8), the value of φ can be found as

$$\phi = \pi/6 \text{ rad}. \tag{9}$$

From (9), it can be observed that the quarter-wave symmetry of the pole voltage waveform V_{HB1} can be maintained if the zero crossing of the carrier lags the voltage reference zero crossing by π/6 rad. Equation (9) gives the value of Φ in terms of the fundamental period of the voltage reference. If the value of Φ is expressed in terms of carrier period, then Φ should be equal to π/2 rad for $p = 3$. In a similar way, the conditions for quarter-wave symmetry at the other intersection points can also be derived and all of them arrive at the same conclusion. Similarly, when the zero crossing of the carrier leads the voltage reference zero crossing by an angle $\Phi = \pi/2$ rad, quarter-wave symmetry among pole voltage waveform V_{HB1} in a single HB can be maintained.

Equation (9) shows the condition for quarter-wave symmetry among pole voltage waveforms V_{HB1}, when $p = 3$. For carriers having frequency $p = 3n$ (where $n = 1, 3, 5, 7, 9$, etc.) times the fundamental frequency and with their zero crossings lagging the fundamental voltage reference zero crossings by Φ rad, the condition for quarter-wave symmetry among pole voltage waveform V_{HB1} can be found by using (10)–(14). Here, for quarter-wave symmetry, the constraint is given by

$$\theta_{6n+1-l} = \pi - \theta_l \quad \text{for l} = 1, 2, \ldots, 3n. \tag{10}$$

For $l = 1$

$$-m \sin \theta_1 = \left(\frac{6n}{\pi}\right)(\theta_1 - \phi) \tag{11}$$

$$m \sin \theta_{6n} = \left(\frac{6n}{\pi}\right)\left\{\theta_{6n} - \phi - \frac{(3n-1)}{3n}\pi\right\}. \tag{12}$$

By putting the constraint of quarter-wave symmetry $\theta_{6n} = \pi - \theta_1$ in (12), one gets

$$m \sin \theta_1 = \left(\frac{6n}{\pi}\right)\left(\frac{\pi}{3n} - \theta_1 - \phi\right). \tag{13}$$

By adding (11) and (13), the value of φ can be found as

$$\phi = \left(\frac{1}{3n}\right)\left(\frac{\pi}{2}\right) \text{ rad}. \tag{14}$$

Hence, by representing Φ in terms of carrier period, it can be concluded that for maintaining quarter-wave symmetry among pole voltage waveform V_{HB1}, the zero crossing of the carrier should lag the zero crossing of the voltage reference by π/2 rad.

In a similar way, conditions for quarter-wave symmetry can be analytically derived for an even integer ratio of carrier and fundamental frequency with zero carrier phase shift, odd integer ratio with zero carrier phase shift, and even integer ratio with π/2 rad phase shift. Therefore, the conditions for maintaining quarter-wave symmetry among pole voltage waveform V_{HB1} in a single HB can be summarized as follows:

1) The zero crossings of the voltage references should coincide with the zero crossings of the carrier.
2) The zero crossings of the carrier should be placed at $\pm\pi/2$ rad with respect to the zero crossings of the voltage references (where 2π rad denotes one carrier period).

If we have only two HBs per phase, then their individual carriers should be phase shifted from each other by π/2 rad. One carrier can satisfy condition I and the other carrier can satisfy condition II as described above. The output voltage of both the HBs will maintain quarter-wave symmetry and hence their sum will also maintain quarter-wave symmetry. But, as the number of cascaded HBs increases (more than two) it is not possible to place all the zero crossings of carriers at 0 or $\pm\pi/2$ rad with respect to the zero crossings of voltage references, as the phase difference between (π/x rad for $x \geq 2$ number of cascaded HBs) zero crossings of the carriers decreases. For two cascaded HBs, the next section deals with the conditions for maintaining quarter-wave symmetry among resultant pole voltage V_{HB}, where the zero crossings of the carriers are placed other than 0 or $\pm\pi$ 2 rad with respect to the voltage reference zero crossings.

2) Two Cascaded H-Bridges: For two cascaded HBs [see Fig. 1(b)], it is also possible to maintain quarter-wave symmetry among the resultant pole voltage waveform V_{HB}, in spite of individual bridge voltage waveforms V_{HB1} and V_{HB2} not maintaining quarter-wave symmetry. Two approaches are possible and pointed below. Both the approaches are analyzed in the coming sections.

1) Zero crossings of carriers C_{HB1} and C_{HB2} are placed on both sides of the zero crossing of carrier C^{ref1} (where C^{ref1} is a fictitious carrier whose zero crossings are in

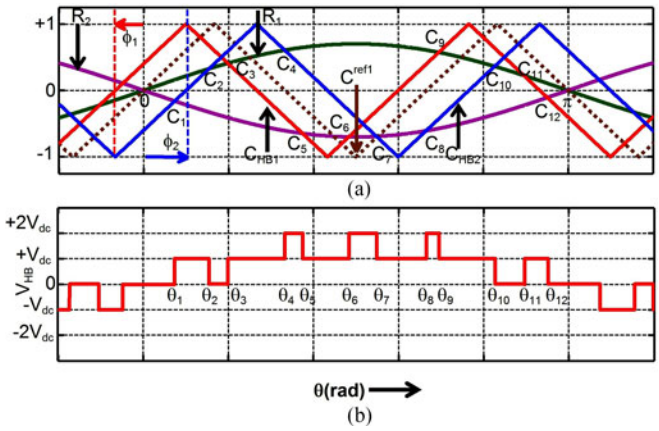

Fig. 4. (a) References R_1 and R_2 and carriers $C_{\rm HB1}$ and $C_{\rm HB2}$ when C^{ref1} is in phase with voltage references ($p = 3$) and (b) $V_{\rm HB}$.

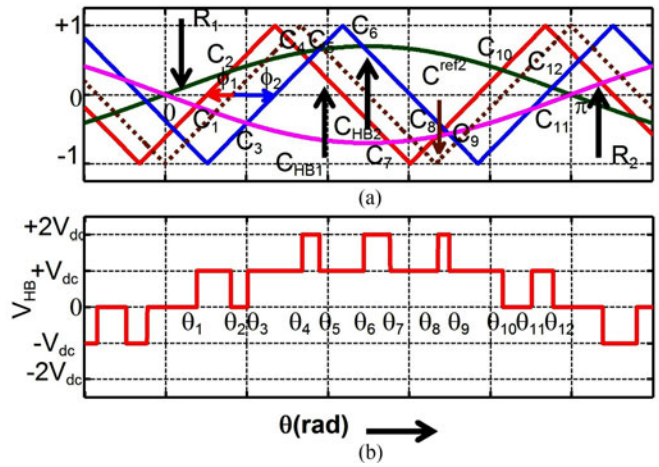

Fig. 5. (a) References R_1 and R_2 and carriers $C_{\rm HB1}$ and $C_{\rm HB2}$ when C^{ref2} is $\pi/2$ rad lagging with respect to voltage references ($p = 3$) and (b) $V_{\rm HB}$.

phase with the zero crossings of the voltage references R_1 and R_2).

2) Zero crossings of carriers $C_{\rm HB1}$ and $C_{\rm HB2}$ are placed on both sides of the zero crossing of carrier C^{ref2} (where C^{ref2} is a fictitious carrier whose one positive or negative peak appears in the same instant as that of the zero crossings of the voltage references R_1 and R_2).

In other words, it can be stated that C^{ref1} satisfies condition I and C^{ref2} satisfies condition II. The carriers $C_{\rm HB1}$ and $C_{\rm HB2}$ are used for generating gate pulses of HB1 and HB2, respectively, in a double cascaded HB [see Fig. 1(b)]. The voltage reference R_1 is used for generating the gate pulses of S_{11}, S_{12}, S_{13}, and S_{14}. The gate pulses of S_{13}, S_{14}, S_{23}, and S_{24} are generated by voltage reference R_2. Figs. 4 and 5 show the voltage references R_1 and R_2 along with carriers $C_{\rm HB1}$ and $C_{\rm HB2}$ with respect to the fictitious carriers C^{ref1} and C^{ref2}, respectively.

a) Approach I: Fig. 4 shows the case where the zero crossing of carrier $C_{\rm HB1}$ leads the zero crossing of fictitious carrier C^{ref1} by Φ_1 rad, whereas the zero crossing of carrier $C_{\rm HB2}$ lags the zero crossing of C^{ref1} by Φ_2 rad for $p = 3$. Fig. 4(b) shows that the resultant pole voltage $V_{\rm HB}$ does not maintain quarter-wave symmetry. In order to show the intersection points and intersection angles, only the half-cycle of each waveform is shown in Fig. 4. For maintaining quarter-wave symmetry of the resulting pole voltage $V_{\rm HB}$, the condition to be satisfied among voltage reference and carrier intersection points C_1–C_{12} is given by

$$\theta_{13-l} = \pi - \theta_l \quad \text{for } l = 1,\ 2,\ 3,\ 4,\ 5, \text{ and } 6. \tag{15}$$

For $l = 1$, the values of θ_1 and θ_{12} at points C_1 and C_{12} can be found out by equating the equations of voltage references and carriers and can be written, respectively, as

$$-m\sin\theta_1 = \left(\frac{6}{\pi}\right)(\theta_1 - \phi_2) \tag{16}$$

$$-m\sin\theta_{12} = -\left(\frac{6}{\pi}\right)(\theta_{12} - \pi + \phi_1). \tag{17}$$

By putting the condition of quarter-wave symmetry (15), (17) can be modified as.

$$m\sin\theta_1 = \left(\frac{6}{\pi}\right)(\phi_1 - \theta_1). \tag{18}$$

By adding (16) and (18), the condition for quarter-wave symmetry can be found out as

$$\phi_1 = \phi_2. \tag{19}$$

From (19) it can be observed that the quarter-wave symmetry among resultant pole voltage waveform $V_{\rm HB}$ can be maintained if $\Phi_1 = \Phi_2$, i.e., the zero crossings of carriers $C_{\rm HB1}$ and $C_{\rm HB2}$ are placed equidistantly from the zero crossings of carrier C^{ref1}. In a similar way, the conditions for quarter-wave symmetry at the other intersection points can also be derived and each pair of intersection points will result in the condition of (19).

Equation (19) shows the condition for quarter-wave symmetry among pole voltage waveform $V_{\rm HB}$, when $p = 3$. For carriers having frequency $p = 3n$ (where $n = 1,\ 2,\ 3,\ 4,\ 5,\ 6,\ 7,\ 8,\ 9,\ 10$, etc.) times the fundamental frequency and with their zero crossings lagging and leading the zero crossing of C^{ref1} by Φ_1 and Φ_2 rad, respectively, the condition for quarter-wave symmetry among resultant pole voltage waveform $V_{\rm HB}$ can be found by using the above-mentioned approaches [see (16)–(19)] and the final conclusion is the same as (19).

b) Approach II: In the second approach (see Fig. 5), the zero crossing of carrier $C_{\rm HB1}$ leads the zero crossing of carrier C^{ref2} by Φ_1 rad, whereas the zero crossing of carrier $C_{\rm HB2}$ lags the zero crossing of carrier C^{ref2} by Φ_2 rad for $p = 3$. Fig. 5(b) shows that the resultant pole voltage $V_{\rm HB}$ does not maintain quarter-wave symmetry. For maintaining quarter-wave symmetry among resultant pole voltage waveform $V_{\rm HB}$, the condition to be satisfied among voltage reference and carrier intersection points C_1–C_{12} is given by

$$\theta_{13-l} = \pi - \theta_l \quad \text{for l} = 1,\ 2,\ 3,\ 4,\ 5, \text{ and } 6. \tag{20}$$

For $l = 1$, the values of θ_1 and θ_{12} at points C_1 and C_{12} can be found out by equating the equations of voltage references

TABLE I
THREE CASCADED H-BRIDGES

Position of $C_{\mathrm{HB}1}$	Position of $C_{\mathrm{HB}2}$	Position of $C_{\mathrm{HB}3}$
$\mp\pi/3$ rad	0 rad	$\pm\pi/3$ rad
$\mp\pi/6$ rad	$\pm\pi/6$ rad	$\pm\pi/2$ rad
$\mp\pi/6$ rad	$\mp\pi/2$ rad	$\mp5\pi/6$ rad
0 rad	$\mp\pi/3$ rad	$\mp2\pi/3$ rad

Zero crossing of voltage reference is placed at 0 rad.

and carriers and can be written, respectively, as

$$-m\sin\theta_1 = \left(\frac{6}{\pi}\right)\left(\theta_1 - \frac{\pi}{6} + \phi_1\right) \tag{21}$$

$$m\sin\theta_{12} = \left(\frac{6}{\pi}\right)\left(\theta_{12} - \frac{5\pi}{6} - \phi_2\right). \tag{22}$$

By putting the condition of quarter-wave symmetry (20) in (22), (22) can be simplified as

$$m\sin\theta_1 = \left(\frac{6}{\pi}\right)\left(\frac{\pi}{6} - \theta_1 - \phi_2\right). \tag{23}$$

By adding (21) and (23), the condition for quarter-wave symmetry can be found out as

$$\phi_1 = \phi_2. \tag{24}$$

From (24) it can be observed that here also the quarter-wave symmetry among resultant pole voltage waveform V_{HB} can be maintained if $\Phi_1 = \Phi_2$, i.e., the zero crossings of carriers C_{HB1} and C_{HB2} are equidistant from the zero crossing of carrier C^{ref2}. The condition of quarter-wave symmetry can also be shown as $\Phi_1 = \Phi_2$, if the zero crossing of carrier C^{ref2} leads π/2 rad from the zero crossing of the voltage references. Same condition for quarter-wave symmetry can be derived for carriers having frequency $p = 3n$ (where $n = 1, 2, 3, 4, 5, 6, 7, 8, 9, 10$, etc.) times the fundamental frequency.

c) Conditions for quarter-wave symmetry with x (≥2) numbers of cascaded H-bridges: From the previous discussions on quarter-wave symmetry, it can be extended that there can be multiple approaches of maintaining quarter-wave symmetry among the resultant pole voltage waveform. For example, if there are two HBs, then one approach can be to put one carrier coinciding with C^{ref1} and the other carrier coinciding with C^{ref2}. Another approach can be to put two carriers such that one carrier leads C^{ref1} (or C^{ref2}) by π/4 rad and the other carrier lags C^{ref1} (or C^{ref2}) by π/4 rad. If there are three cascaded HBs, then the possible approaches are given as Table I. Hence, it is important to determine the general philosophy of placing the carriers with respect to the voltage reference to ensure quarter-wave symmetry for a $(2x + 1)$-level cascaded HB MLI (x number of cascaded HBs). The philosophy is analytically explained in this section. For this analysis, position of a carrier is defined by the position of the zero crossing of the carrier.

Case I: [With one carrier being at $0\mathrm{th}$ position ($0\mathrm{th}$ carrier), k numbers of carriers are present on the left-hand side (between points A and B) and $(x-k-1)$ numbers of carriers are present on the right-hand side (between points D and H) of the 0th carrier]. It is to be noted that the zero crossing of voltage reference *R* coincides with the zero crossing of the carrier placed at $0\mathrm{th}$ position.

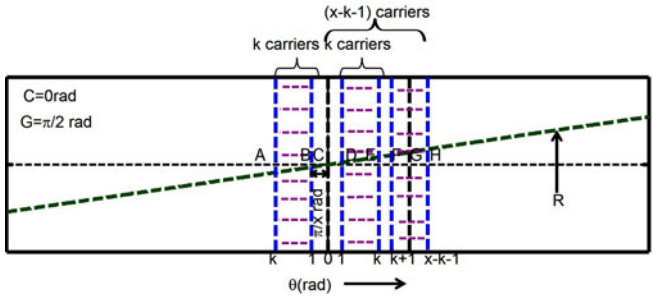

Fig. 6. Positive zero crossing (point C) of normalized voltage reference *R* coincides with the positive zero crossing (point C) of $0\mathrm{th}$ carrier.

Fig. 6 shows case I, where k numbers of carriers are present on the left-hand side of $0\mathrm{th}$ carrier and $(x - k - 1)$ numbers of carriers are present on the right-hand side of $0\mathrm{th}$ carrier. The zero crossings of each carrier are separated from each other by π/x rad. The positive zero crossing of the normalized voltage reference *R* coincides with the positive zero crossing of $0\mathrm{th}$ carrier. It can also be observed from Fig. 6 that equal numbers (k numbers) of carriers are present around point C between points A–B and D–E. Hence, the resultant output pole voltage waveform of the HBs using these carriers maintains quarter-wave symmetry. Also, the pole voltage output of the HB using $0\mathrm{th}$ carrier maintains quarter-wave symmetry. Hence, for maintaining quarter-wave symmetry among the resultant pole voltage waveform of x numbers of cascaded HBs, it should be shown that the positive zero crossings of $(k+1)\mathrm{th}$ and $(x-k-1)\mathrm{th}$ carriers [among $(x - 2k - 1)$ carriers between points F–H] are present equidistantly from π/2 rad (point G).

The distances between points G–F and H–G are calculated as

$$\mathrm{FG} = \frac{\pi}{2} - (k+1) * \left(\frac{\pi}{x}\right) = \left(\frac{x-2k-2}{2}\right) * \left(\frac{\pi}{x}\right) \tag{25}$$

$$\mathrm{GH} = (x-k-1) * \left(\frac{\pi}{x}\right) - \frac{\pi}{2} = \left(\frac{x-2k-2}{2}\right) * \left(\frac{\pi}{x}\right). \tag{26}$$

Equations (25) and (26) show that the positive zero crossings of $(k+1)\mathrm{th}$ and $(x-k-1)\mathrm{th}$ carriers are placed equidistantly from π/2 rad.

The above-mentioned explanation can be extended to even/odd numbers of cascaded HBs. For an even number of cascaded HBs one carrier is present at π/2 rad and equal numbers of carriers are present on both sides of π/2 rad. For an odd number of cascaded HBs no carrier is present at π/2 rad and equal numbers of carriers are present on both sides of π/2 rad.

Case II [k numbers of carriers are present on the left-hand side (between points A and B) and $(x - k)$ numbers of carriers are present on the right-hand side (between points D and H) of the point C (the midpoint of points B and D) and the positive

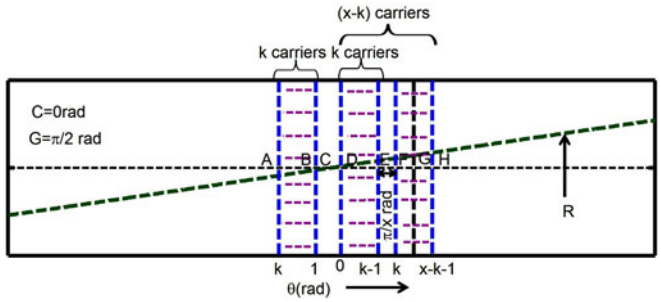

Fig. 7. Positive zero crossing (point C) of normalized pole voltage reference *R* is placed in between the positive zero crossings (points B and D of two adjacent carrier pairs).

zero crossing of voltage reference *R* coincides with point C]. There is no 0th carrier in this case.

Fig. 7 shows case II, where *k* numbers of carriers are present on the left-hand side of point *C* and (*x* – *k*) numbers of carriers are present on the right-hand side of point C. The zero crossings of each carrier are separated from each other by π/x rad. The positive zero crossing of the normalized voltage reference *R* coincides with the point C (midpoint of the two adjacent carriers). It also can be observed from Fig. 7 that equal numbers (*k* numbers) of carriers are present around point C between points A–B and D–E. Hence, the resultant output pole voltage waveform of the HBs using these carriers maintains quarter-wave symmetry. For maintaining quarter-wave symmetry among the resultant pole voltage waveform of *x* numbers of cascaded HBs, it should be shown that the positive zero crossings of $k\text{th}$ and $(x-k)\text{th}$ carriers (among *n* – 2 *k* carriers between points F and H) are present equidistantly from $\pi/2$ rad (point G).

The distances between points G–F and H–G are calculated as

$$\text{FG} = \frac{\pi}{2} - \left\{k * \left(\frac{\pi}{x}\right) + \frac{\pi}{2x}\right\} = \left(\frac{x-2k-1}{2}\right) * \left(\frac{\pi}{x}\right) \quad (27)$$

$$\text{GH} = \left\{(x-k-1) * \left(\frac{\pi}{x}\right) + \frac{\pi}{2x}\right\} - \frac{\pi}{2} = \left(\frac{x-2k-1}{2}\right) * \left(\frac{\pi}{x}\right). \quad (28)$$

Equations (27) and (28) show that the positive zero crossings of $k\text{th}$ and $(x-k)\text{th}$ carriers are placed equidistantly from $\pi/2$ rad.

The above-mentioned explanation can be extended to even/odd numbers of cascaded HBs. For an even number of cascaded HBs no carrier is present at $\pi/2$ rad and equal numbers of carriers are present on both sides of $\pi/2$ rad. For an odd number of cascaded HBs, one carrier is present at $\pi/2$ rad and equal numbers of carriers are present on both sides of $\pi/2$ rad.

d) Generalized condition for maintaining quarter-wave symmetry: Table II summarizes the conditions to maintain quarter-wave symmetry among resultant pole voltage waveform for x ($x \geq 2$) numbers of the cascaded HB inverter. It is to be noted that it is required to satisfy any one condition mentioned in Table II in order to maintain quarter-wave symmetry. It is observed that if any one of these conditions is maintained, then leaving out the in-phase and $\pi/2$ rad-phase carriers (if they exist),

TABLE II
x CASCADED H-BRIDGE MULTILEVEL INVERTERS

	CONDITION FOR QUARTER-WAVE SYMMETRY $f_c/f_s = 3n$ (where $n = 1, 2, 3, 4$, etc.)
1	Zero crossing of voltage reference coincides with zero crossing of any carrier
2	Zero crossing of voltage reference is placed at the midpoint between positive (or negative) zero crossings of any two adjacent carriers

There are *x* phase-shifted carriers with π/x phase difference between any two adjacent carriers.

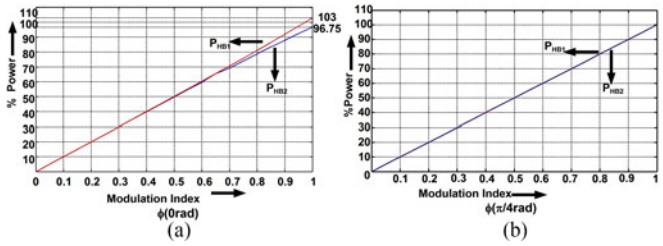

Fig. 8. Power distribution between each H-bridge of a five-level CHBMLI (a) Positive zero crossing of C_{HB1} coincides with the zero crossings of R_1 and R_2 and (b) zero crossings of R_1 and R_2 are placed at $\pm\pi$ 4 rad with respect to the zero crossings of C_{HB1} and C_{HB2} for $p = 3$.

equal number of carriers will be placed on both sides of C^{ref1} (as shown in Fig. 4) or C^{ref2} (as shown in Fig. 5) or both.

e) Power distribution between each cell: For the PSPWM technique with a high switching frequency, each HB handles equal power. But when the ratio *p* becomes low, unequal power distribution occurs between the cascaded HBs. The reason is the same current passes through each module. But, their instantaneous output voltage waveforms are different. Hence, the instantaneous power integrated over a complete fundamental cycle may result is different values. Fig. 8 shows that when the zero crossings of the voltage references coincide with the zero crossing of one of the carriers, condition of unequal distribution of power between the HBs occurs. But when the zero crossings of the voltage references are placed equidistantly between the zero crossings of the two carriers, then each HB shares equal power. It is to be noted that this is just a specific example. In general, *x* CHBMLIs unequal power distribution may occur for lesser value of *p*.

f) Fundamental displacement and harmonic distortion without maintaining QWS: In order to study the importance of maintaining quarter-wave symmetry (QWS), with $p = 3$, the angle Φ (distance between the zero crossing of voltage reference and the positive zero crossing of C_{HB1}) is varied in HB1 [see Fig. 1(b)] from 0 to $\pi/6$ rad (0 to $\pi/2$ rad in terms of carrier period). Hence, the positive zero crossing of C_{HB2} varies from $\pi/6$ to $\pi/3$ rad with respect to the fundamental reference ($\pi/2$ to π rad in terms of carrier period). Fig. 9(a) shows that for a single HB (HB1), maximum phase displacement (α_{HB1}) occurs between the voltage reference and the fundamental of pole voltage for $\Phi = \pi/4$ rad (in terms of carrier period). At both the extreme ends, i.e., at $\Phi = 0$ rad (condition of QWS) and $\Phi = \pi/2$ rad (condition of QWS), the phase displacements are zero. Similarly, Fig. 9(b) shows at $\Phi = 0$ rad (condition of

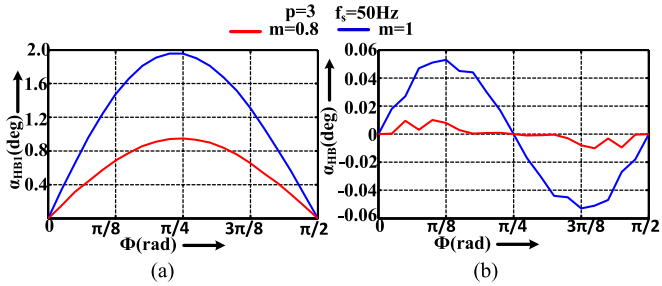

Fig. 9. Fundamental voltage displacements of (a) single H-bridge and (b) double cascaded H-bridges for $p = 3$, $f_s = 50$ Hz, and with modulation indexes of 0.8 and 1.

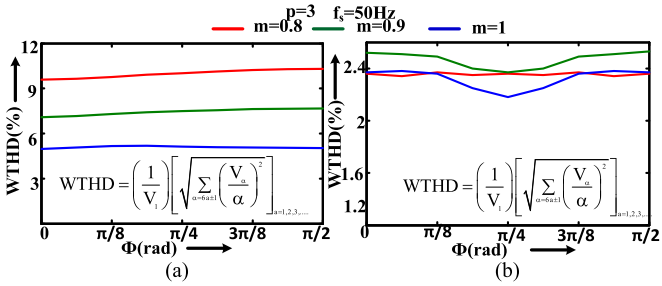

Fig. 10. WTHD (line voltage V_{RY}) variations with respect to the variation of Φ for higher modulation indexes (0.8 to 1) for (a) single H-bridge and (b) double cascaded H-bridges with $p = 3$, $f_s = 50$ Hz.

QWS), $\Phi = \pi$ 4 rad (condition of QWS) and $\Phi = \pi$ 2 rad (condition of QWS), the phase displacements are zero for the double cascaded HBs. Fig. 9 also shows that the phase displacement for a single HB is higher comparing to the double cascaded HBs. If the number of cascaded HBs are further increased, then the phase displacement reduces to lesser values and hence, for a very large number of cascaded HB cells, with phase-shifted carriers, phase displacement of the resultant pole voltage is negligible even without perfect quarter-wave symmetry.

In order to check the variation of the harmonic profile of the line voltage with respect to the variation of Φ (distance between the zero crossing of voltage reference and the positive zero crossing of C_{HB1}), the weighted THD (WTHD) plots for line voltage V_{RY} are plotted in Fig. 10 for a three-level (single HB) and five-level (two cascaded HBs) CHBMLI, for three modulation indexes 0.8, 0.9, and 1, with $p = 3$ and $f_s = 50$ Hz. For single HB, the positions $\Phi = 0$ and $\pi/2$ rad are the conditions for quarter-wave symmetry whereas for two cascaded HBs, the positions 0, $\pi/4$, and $\pi/2$ rad are the conditions of maintaining QWS among pole voltage waveform. Here, it can be observed that for a single HB, WTHD varies almost in a flat profile. For two cascaded HBs, for higher modulation indexes, minimum WTHD occurs at $\Phi = \pi$ 4 rad (i.e., the zero crossing of voltage reference is placed at the midpoint of the zero crossings of two carriers) which is a valid condition for quarter-wave symmetry. The improvement is of course too small for consideration in a practical situation.

The proposed PSPWM technique does not give a better harmonic voltage profile compared to the techniques proposed in [8], [20], and [21], as the gate pulses are generated without any

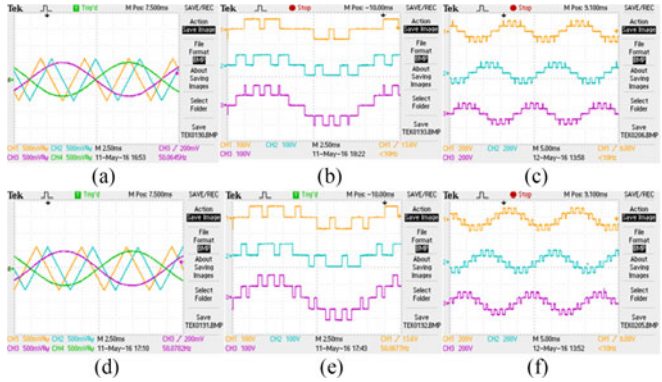

Fig. 11. (a) and (d) Ch.1:$-C_{\mathrm{HB1}}$, Ch.2:$-C_{\mathrm{HB2}}$, Ch.3:$-R_1$, and Ch.4:$-R_2$; (b) and (e) Ch.1:$-V_{\mathrm{HB1}}$, Ch.2:$-V_{\mathrm{HB2}}$, and Ch.3:$-V_{\mathrm{HB}}$, and (c) and (f) Ch.1:$-V_{\mathrm{RO}}$, Ch.2:$-V_{\mathrm{BO}}$, and Ch.3:$-V_{\mathrm{YO}}$ when (i) the zero crossings of voltage references are in phase with the zero crossings of carrier C_{HB1} and (ii) the zero crossings of voltage references are placed at the midpoint of the positive zero crossings of carriers C_{HB1} and C_{HB2} for $f_c = 3\,f_s$ with a modulation index of 0.8 and $f_s = 50$ Hz.

harmonic minimization technique. Edpuganti *et al.* [8], [21] show the applications of the SOPWM technique, where the switching instants are calculated for minimizing certain voltage harmonics along with minimization of current distortion. Tripathi and Narayanan [20] calculate the switching instants by minimizing the required voltage harmonics along with the constraint of minimizing the pulsating torque. The proposed PSPWM technique does not claim to give reduced current or torque ripple. But it can be stated that with lower p and reduced number of HBs, the proposed PSPWM technique gives better performance compared to the traditional PSPWM technique (the zero crossings of voltage references can be put arbitrarily irrespective of zero crossings of the phase-shifted carriers). Furthermore, as the proposed technique is a carrier-based scheme, synchronization in a highly dynamic situation such as field-oriented control can be achieved with much lesser computational complexity compared to the schemes of [8], [20], [21], etc. But, with the increase in the number of HBs and p, the harmonic profile is almost similar to a traditional PSPWM technique [22]–[25].

III. Experimental Results

The synchronization strategy for the CHBMLIs is verified with a three-phase squirrel cage induction motor drive (parameters are given in the Appendix) operated in an open loop *V/f* mode, which is supplied from a five-level three-phase CHBMLI laboratory prototype. The dc-link voltage V_{dc} of each HB is maintained at 100 V during the experiment to operate the motor at half of the rated voltage. Both the conditions for maintaining quarter-wave symmetry in the resultant pole voltage patterns V_{HB}, as discussed in Section II, are tested experimentally. For experimental verification, the ratio p is kept at three in order to show the pole voltage pulse patterns clearly. Fig. 11(a) shows that the zero crossings of carrier C_{HB1} coincide with the zero crossings of voltage references R_1 and R_2. Fig. 11(b) shows that the individual bridge voltage waveforms V_{HB1} and V_{HB2} along with the resultant pole voltage waveform V_{HB} maintain half-wave symmetry and quarter-wave symmetry. Fig. 11(d)

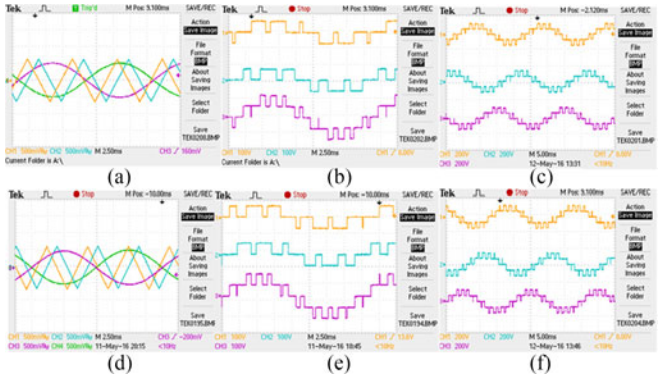

Fig. 12. (a) and (d) Ch.1:$-C_{\mathrm{HB1}}$, Ch.2:$-C_{\mathrm{HB2}}$, Ch.3:$-R_1$, and Ch.4:$-R_2$; (b) and (e) Ch.1:$-V_{\mathrm{HB1}}$, Ch.2:$-V_{\mathrm{HB2}}$, and Ch.3:$-V_{\mathrm{HB}}$, and (c) and (f) Ch.1:$-V_{\mathrm{RO}}$, Ch.2:$-V_{\mathrm{BO}}$, and Ch.3:$-V_{\mathrm{YO}}$ when (i) the zero crossings of voltage references are placed at $+\pi/12$ rad with respect to the zero crossings of carrier C_{HB1} for $f_c = 3f_s$ with a modulation index of 0.8 and $f_s = 50$ Hz and (ii) for $f_c = 160$ Hz with a modulation index of 0.8 and $f_s = 50$ Hz.

shows that the zero crossings of voltage references R_1 and R_2 are placed equidistantly in between the zero crossings of carrier C_{HB1} and C_{HB2}. Fig. 11(e) shows the individual bridge voltages V_{HB1} and V_{HB2} and resultant pole voltage V_{HB}. It can be observed that the individual bridge voltages maintain half-wave symmetry, but not quarter-wave symmetry, whereas the resultant pole voltage waveform maintains half-wave symmetry and quarter-wave symmetry. Fig. 11(c) and (f) shows that the three-phase symmetry is maintained among three-phase pole voltage waveforms.

In order to compare the proposed PSPWM technique, the experiment is done with two sets of carriers C_{HB1} and C_{HB2} where the zero crossings of voltage references R_1 and R_2 are placed at an angle of $+\pi$ 12 rad with respect to the zero crossing of C_{HB1}. The ratio p is kept at 3. This condition ensures the three-phase symmetry and half-wave symmetry. But quarter-wave symmetry is not maintained. Fig. 12(a) shows the above-mentioned conditions for voltage references R_1 and R_2 and carriers C_{HB1} and C_{HB2}. Fig. 12(b) shows that the individual bridge voltages V_{HB1} and V_{HB2} along with resultant bridge voltage V_{HB} maintain half-wave symmetry without maintaining quarter-wave symmetry. Fig. 12(c) shows the three-phase pole voltages maintain three-phase symmetry. Similarly, a pair of carriers C_{HB1} and C_{HB2} having frequency of 160 Hz (asynchronous PWM) are used to generate the same waveforms. The results are shown in Fig. 12(d)–(f). It can be observed that the individual bridge voltages along with the resultant bridge voltage do not maintain half-wave symmetry, quarter-wave symmetry, or three-phase symmetry. During the experiment, the modulation index of the voltage references is kept at 0.8 with a frequency of 50 Hz.

The harmonic spectra of line voltages (V_{RY}) with and without waveform symmetries and synchronization are compared in Figs. 13 and 14. Fig. 13(b) and (d) shows the harmonic spectrum of line voltage V_{RY} which is the result of maintaining quarter-wave symmetry for one of the conditions mentioned in Table II. Fig. 14(b) shows the harmonic spectrum of the line voltage V_{RY}, when there is no QWS present among the pole voltage waveform. The harmonic spectra of Figs. 13(b), (d), and 14(b) are free from even-order voltage harmonics, as the pole voltage

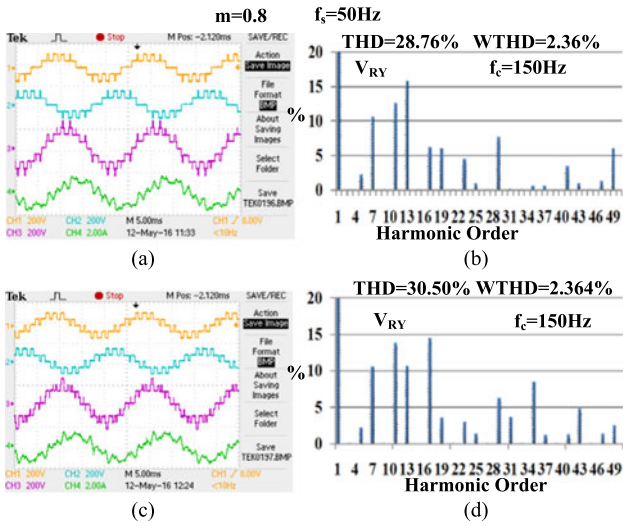

Fig. 13. (a) and (c) Ch.1:$-V_{\mathrm{RO}}$, Ch.2:$-V_{\mathrm{YO}}$, Ch.3:$-V_{\mathrm{RY}}$, and Ch.4:-i_R; (b) and (d) harmonic spectrum of V_{RY} for (i) the zero crossings of voltage references are in phase with the zero crossings of carrier C_{HB1} and (ii) the zero crossings of voltage references are placed at the midpoint of the positive zero crossings of carriers C_{HB1} and C_{HB2} for $f_c = 3f_s$ with a modulation index of 0.8 and $f_s = 50$ Hz.

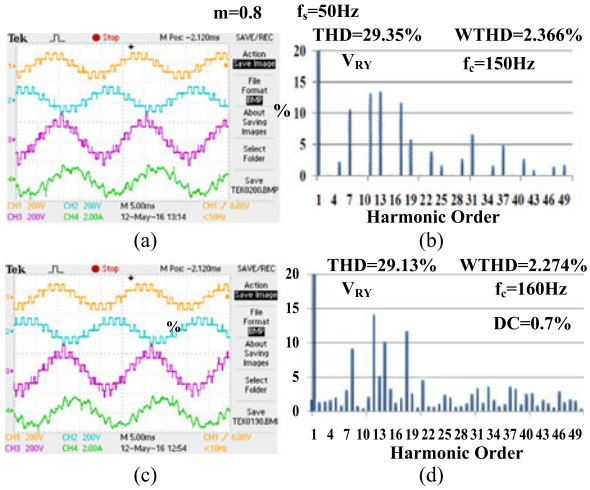

Fig. 14. (a) and (c) Ch.1:$-V_{\mathrm{RO}}$, Ch.2:$-V_{\mathrm{YO}}$, Ch.3:$-V_{\mathrm{RY}}$, and Ch.4:$-i_R$; (b) and (d) harmonic spectrum of V_{RY} for (i) the zero crossings of voltage references are placed at $+\pi$ 12 rad with respect to the zero crossings of carrier C_{HB1} for $f_c = 3f_s$ and (ii) $f_c = 160$ Hz with a modulation index of 0.8 and $f_s = 50$ Hz.

waveform maintains half-wave symmetry (HWS). The harmonic spectra of Figs. 13(b), (d), and 14(b) show that the line voltage is free from triplen-order voltage harmonics. Hence, the three-phase symmetry is maintained among the three-phase pole voltage waveforms. The WTHD of line voltage V_{RY} for the above-mentioned three cases is almost equal. The minor difference is already shown in Fig. 10. Fig. 14(d) shows that the harmonic spectrum of the line voltage V_{RY} contains a small dc offset for 160 Hz phase-shifted carriers. This dc offset is observed in the harmonic spectrum, as the harmonic spectra are plotted for one fundamental cycle. For an asynchronous carrier, the pole voltage waveform along with the line voltage waveform is not periodic considering one fundamental period of the

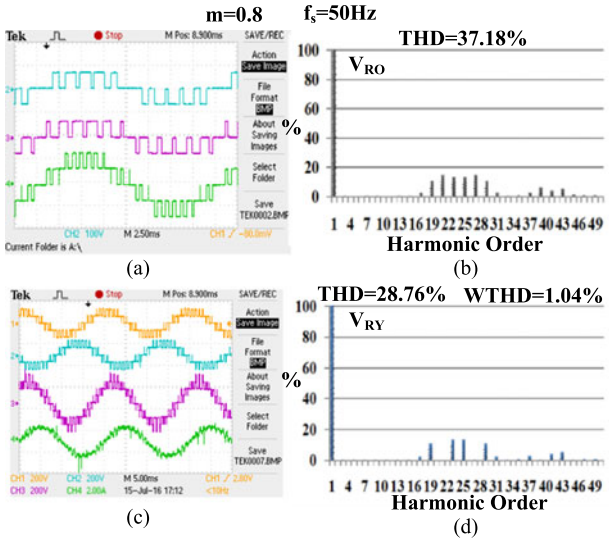

Fig. 15. (a) Ch.2:$-V_{\mathrm{HB1}}$, Ch.3:$-V_{\mathrm{HB2}}$, and Ch.4:$-V_{\mathrm{HB}}$; (b) harmonic spectrum of V_{RO}; (c) Ch.1:$-V_{\mathrm{RO}}$, Ch.2:$-V_{\mathrm{YO}}$, Ch.3:$-V_{\mathrm{RY}}$, and Ch.4:$-i_R$, and (d) harmonic spectrum of V_{RY} when the zero crossings of voltage references are in phase with the zero crossings of carrier C_{HB1} for $f_c = 6f_s$ with a modulation index of 0.8 and $f_s = 50$ Hz.

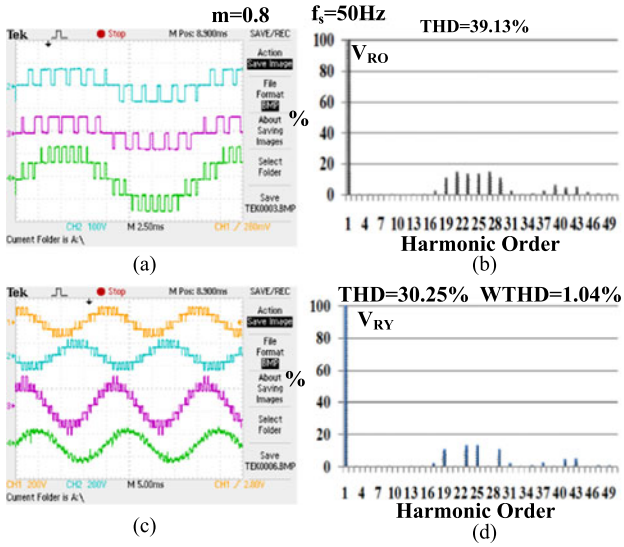

Fig. 16. (a) Ch.2:$-V_{\mathrm{HB1}}$, Ch.3:$-V_{\mathrm{HB2}}$, and Ch.4:$-V_{\mathrm{HB}}$; (b) harmonic spectra of V_{RO}; (c) Ch.1:$-V_{\mathrm{RO}}$, Ch.2:$-V_{\mathrm{YO}}$, Ch.3:$-V_{\mathrm{RY}}$, and Ch.4:$-i_R$, and (d) harmonic spectra of V_{RY} when the zero crossings of voltage references are placed at the midpoint of the zero crossings of carriers C_{HB1} and C_{HB2} for $f_c = 6f_s$ with a modulation index of 0.8 and $f_s = 50$ Hz.

voltage reference. But, if the harmonic spectra are plotted based on a data of a time period in which both the fundamental and the carriers complete integer number of cycles, then this dc offset will not be observed in the harmonic spectra of pole voltage as well as line voltage. Rather, it will appear as subharmonic component. The subharmonic frequency is very bad for drive's application, because it may match with the mechanical resonance frequency of the drive shaft. Moreover, it is a common practice to use inverter output filters for drives with long distance between the converter and the motor. It can be observed that the frequency spectrum with synchronized carrier is of concentrated nature, whereas with asynchronous carrier is of distributed nature. Hence, design of output filter is more economical for a synchronized carrier-based approach where the ratio between the carrier frequency and the fundamental frequency (p) is very low. Also, with asynchronous carriers even-order voltage harmonics are observed in the line voltage waveform, due to the absence of HWS among pole voltage waveform.

Some experimental results are also taken for a three-phase five-level CHBMLI-fed squirrel cage induction motor drive with $p = 6$ and $f_s = 50$ Hz. This experiment is done in order to show that the proposed PSPWM technique is also valid for carriers having a frequency ratio p being even. Figs. 15(a) and 16(a) show the individual bridge voltages along with the resultant bridge voltage of a single-phase five-level CHBMLI with the conditions for maintaining QWS among pole voltage V_{HB} (as mentioned in Table II). Fig. 15(a) shows that the individual bridge voltages along with the resultant bridge voltage maintain HWS and QWS, when the zero crossing of one carrier coincides with the zero crossing of voltage references. Fig. 16(a) shows the individual bridge voltages do not maintain QWS but the resultant bridge voltage maintains QWS when the zero crossing of the voltage references are placed at the midpoint of the zero crossings of the carriers.

Figs. 15 and 16 also show the fast Fourier transform spectra of pole voltage V_{RO} and line voltage V_{RY} for $p = 6$ and $f_s = 50$ Hz with a modulation index of 0.8. The harmonic spectra of pole voltage V_{RO} in Figs. 15(b) and 16(b) show that even-order voltage harmonics are absent. This signifies the pole voltage waveform V_{RO} maintains HWS. The harmonic spectra of line voltage V_{RY} in Figs. 15(d) and 16(d) show the triplen harmonics are absent from the line voltage waveform V_{RY}. This shows that the three-phase pole voltage waveforms maintain three-phase symmetry. The THD of all waveforms are calculated and WTHD is also shown for line voltage V_{RY}. The WTHD of the line voltage V_{RY} shows that the effect of lower order voltage harmonics is identical under both the conditions mentioned in Table II. This occurs as with higher p, the WTHDs of line voltages are almost identical irrespective of the different conditions for maintaining QWS.

Figs. 17 and 18 are taken with the help of a three-phase five-level CHBMLI-fed squirrel cage induction motor drive (during the open loop *V/f* control). Fig. 17 also shows the results for maintaining quarter-wave symmetry among the resultant pole voltage waveform for double cascaded HBs with $p = 9$. Hence, the conditions tabulated in Table II are valid for any $3n$ (where $n = 1, 2, 3$, etc.) carrier. Fig. 18(b) shows the transition of the R-phase current i_R during the shifting between the synchronous carriers having $p = 9$–3. Fig. 18(b) shows a smooth transition between the carriers having $p = 9$–3, as no significant transients are observed in motor current i_R. The results of Fig. 18 are taken when the zero crossings of voltage references are placed at the midpoint of the positive zero crossings of carriers C_{HB1} and C_{HB2}. This approach is selected for experimental verification as the power handled by each bridge is equal for lower p and higher values of modulation indexes as discussed in Section II.

In order to compare the proposed PSPWM technique for higher number of cascaded HBs, the experiment is also per-

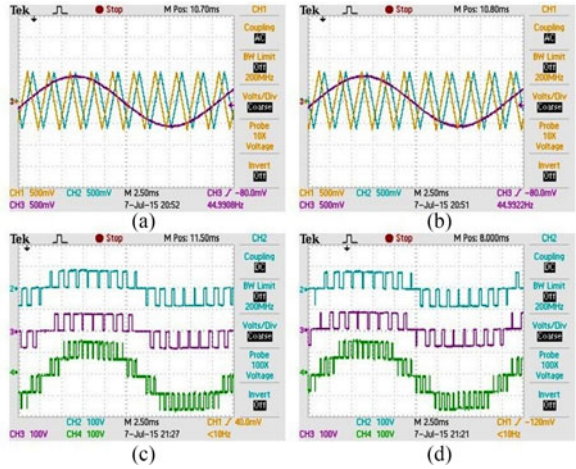

Fig. 17. (a) and (b) Ch.1:$-C_{\mathrm{HB1}}$, Ch.2:$-C_{\mathrm{HB2}}$, Ch.3:$-R_1$, and Ch.4:$-R_2$ and (c) and (d) Ch.1:$-V_{\mathrm{HB1}}$, Ch.2:$-V_{\mathrm{HB2}}$, and Ch.3:$-V_{\mathrm{HB}}$ when (i) the zero crossings of voltage references are placed at the midpoint of the positive zero crossings of carriers C_{HB1} and C_{HB2} and (ii) the zero crossings of voltage references are in phase with the zero crossings of carrier C_{HB2} for $f_c = 9f_s$ with a modulation index of 0.9 and $f_s = 45$ Hz.

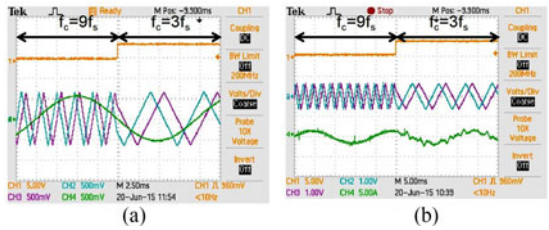

Fig. 18. (a) Ch.1:-Transition signal, Ch.2:$-C_{\mathrm{HB1}}$, Ch.3:$-C_{\mathrm{HB2}}$, and Ch.4:-R-phase voltage reference and (b) Ch.1:-transition signal, Ch.2:$-C_{\mathrm{HB1}}$, Ch.3:$-C_{\mathrm{HB2}}$, and Ch.4:-i_R during the transition from $p = 9$ to 3.

formed with a nine-level CHBMLI. Fig. 19 shows the results for two possible combinations of placement of zero crossings of voltage references with respect to the positive zero crossings of the carriers. Fig. 19(a) and (b) shows the waveforms of individual bridge voltages along with the resultant bridge pole voltage, respectively, when the zero crossing of voltage reference coincides with the positive zero crossing of one of the carriers. Fig. 19(d) and (e) shows the waveforms of individual bridge voltages along with the resultant bridge pole voltage, respectively, when the zero crossing of voltage references is placed at the midpoint of the positive zero crossings of two adjacent carriers. The harmonic spectra of pole voltage waveform V_{RO} are shown in Fig. 19(c) and (f). The even-order harmonics are eliminated from the harmonic spectrum of the pole voltage waveform, as all the waveforms maintain HWS. It can be stated that with the increase in the number of voltage levels, the harmonic spectrum is shifted to higher orders and their magnitude also comes down. All the plots are done for a modulation index (m) of 0.8 at a pole voltage reference frequency (f_s) of 50 Hz and $p = 3$.

IV. Conclusion

This paper shows analytically the possible positions of zero crossings of the carriers with respect to the zero crossings of

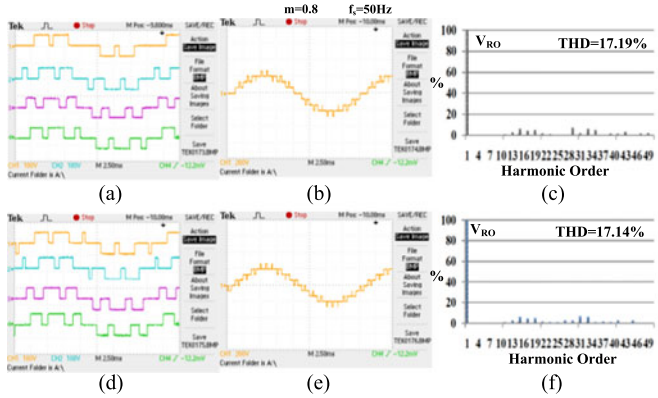

Fig. 19. (a) and (d) Ch.1:$-V_{\mathrm{HB1}}$, Ch.2:$-V_{\mathrm{HB2}}$, Ch.3:$-V_{\mathrm{HB3}}$, and Ch.4:$-V_{\mathrm{HB4}}$; (b) and (e) Ch.1:$-V_{\mathrm{HB}}$, and (c) and (f) harmonic spectrum of V_{HB} when (i) the positive zero crossing of one carrier coincides with the zero crossing of fundamental voltage reference and (ii) the zero crossing of fundamental voltage reference is placed at the midpoint of two adjacent carriers with a modulation index of 0.8, $f_s = 50$ Hz, and $p = 3$ for a single-phase nine-level CHBMLI.

voltage references for the CHBMLIs using the PSPWM technique for maintaining three-phase symmetry, half-wave symmetry, and quarter-wave symmetry. Three-phase and half-wave symmetries are maintained among the HB pole voltage waveforms for any position of zero crossing of carrier with respect to the zero crossing of the voltage references, as long as carrier frequency is $3n$ time the fundamental frequency with n being any integer (even/odd). But the positions of zero crossings of the carriers with respect to the zero crossings of voltage references are important for maintaining quarter-wave symmetry among the pole voltage waveforms. This is analytically studied in this paper for single and two cascaded HBs and generalized for x number of cascaded HBs. The study is experimentally verified with the help of a three-phase five-level CHBMLI laboratory prototype and the results are presented.

Appendix

A. Squirrel Cage Induction Motor Parameters

Stator phase voltage (V)	400
Rated supply frequency (Hz)	50
Stator phase current (A)	7.7
Shaft power (kW)	3.73
Pole pairs	3
Full load rated speed (r/min)	960
Magnetizing inductance (mH)	190
Stator and rotor leakage inductance (mH)	8.8
Stator resistance (Ω)	0.9
Rotor resistance (Ω)	0.78
Rotor inertia (kgm^2)	0.1
Viscous coefficient (Nm/rad/s)	0.003

References

[1] J. Rodriguez, S. Bernet, B. Wu, J. O. Pontt, and S. Kouro, "Multilevel voltage-source-converter topologies for industrial medium-voltage drives," *IEEE Trans. Ind. Electron.*, vol. 54, no. 6, pp. 2930–2945, Dec. 2007.

[2] H. Abu-Rub, J. Holtz, J. Rodriguez, and Ge Baoming, "Medium-voltage multilevel converters—State of the art, challenges, and requirements in industrial applications," *IEEE Trans. Ind. Electron.*, vol. 57, no. 8, pp. 2581–2596, Aug. 2010.

[3] S. Kouro *et al.*, "Recent advances and industrial applications of multilevel converters," *IEEE Trans. Ind. Electron.*, vol. 57, no. 8, pp. 2553–2580, Aug. 2010.
[4] G. Narayanan and V. T. Ranganathan, "Two novel synchronized bus-clamping PWM strategies based on space vector approach for high power drives," *IEEE Trans. Power. Electron.*, vol. 17, no. 1, pp. 84–93, Jan. 2002.
[5] A. R. Beig, S. Kanukollu, K. Al Hosani, and A. Dekka, "Space-vector-based synchronized three-level discontinuous PWM for medium-voltage high-power VSI," *IEEE Trans. Ind. Electron.*, vol. 61, no. 8, pp. 3891–3901, Aug. 2014.
[6] G. Narayanan, "Synchronised pulsewidth modulation strategies based on space vector approach for induction motor drives," Ph.D. dissertation, Indian Inst. Sci., Bangalore, India, 1999.
[7] G. S. Buja and G. B. Indri, "Optimal pulsewidth modulation for feeding AC motors," *IEEE Trans. Ind. Appl.*, vol. IA-13, no. 1, pp. 38–44, Jan./Feb. 1977.
[8] A. Edpuganti and A. K. Rathore, "Optimal low-switching frequency pulsewidth modulation of medium voltage seven-level cascade-5/3 H inverter," *IEEE Trans. Power Electron.*, vol. 30, no. 1, pp. 496–503, Jan. 2015.
[9] A. K. Rathore, J. Holtz, and T. Boller, "Synchronous optimal pulsewidth modulation for low-switching-frequency control of medium-voltage multilevel inverters," *IEEE Trans. Ind. Electron.*, vol. 57, no. 7, pp. 2374–2381, Jul. 2010.
[10] J. Holtz and N. Oikonomou,"Synchronous optimal pulsewidth modulation and stator flux trajectory control for medium-voltage drives," *IEEE Trans. Ind. Appl.*, vol. 43, no. 2, pp. 600–608, Mar./Apr. 2007.
[11] T. Geyer, N. Oikonomou, G. Papafotiou, and F. D. Kieferndorf, "Model predictive pulse pattern control," *IEEE Trans. Ind. Appl.*, vol. 48, no. 2, pp. 663–676, Mar./Apr. 2012.
[12] L. K. Haw, M. S. A. Dahidah, and A. F. A. Haider, "SHE-PWM cascaded multilevel inverter with adjustable dc voltage levels control for STATCOM applications," *IEEE Trans. Power Electron.*, vol. 29, no. 12, pp. 6433–6444, Dec. 2014.
[13] J. Napoles, J. I. Leon, R. Portillo, L. G. Franquelo, and M. A. Aguirre, "Selective harmonic mitigation technique for high-power converters," *IEEE Trans. Ind. Appl.*, vol. 57, no. 7, pp. 2315–2323, Jul. 2010.
[14] Y. Zhang, Y. W. Li, N. R. Zargari, and Z. Cheng, "Improved selective harmonics elimination scheme with online harmonic compensation for high-power PWM converters," *IEEE Trans. Power Electron.*, vol. 30, no. 7, pp. 3508–3517, Jul. 2015.
[15] H. Zhou, Y. W. Li, N. R. Zargari, Z. Cheng, R. Ni, and Y. Zhang, "Selective harmonic compensation (SHC) PWM for grid-interfacing high-power converters," *IEEE Trans. Power Electron.*, vol. 29, no. 3, pp. 1118–1127, Mar. 2014.
[16] D. Ahmadi and J. Wang, "Online selective harmonic compensation and power generation with distributed energy resources," *IEEE Trans. Power Electron.*, vol. 29, no. 7, pp. 3738–3747, Jul. 2014.
[17] S. K. Sahoo and T. Bhattacharya, "Synchronization strategies in cascaded H-Bridge multi level inverters for carrier based sinusoidal PWM techniques," in *Proc. 31st Annu. IEEE Appl. Power Electron. Conf. Expo.*, 2016, pp. 199–206.
[18] S. K. Sahoo, T. Bhattacharya, and M. Aravind, "A synchronized sinusoidal PWM based rotor flux oriented controlled induction motor drive for traction application," in *Proc. 28th Annu. IEEE Appl. Power Electron. Conf. Expo.*, Mar. 2013, pp. 797–804.
[19] S. K. Sahoo and T. Bhattacharya, "Rotor flux-oriented control of induction motor with synchronized sinusoidal PWM for traction application," *IEEE Trans. Power Electron.*, vol. 31, no. 6, pp. 4429–4439, Jun. 2016.
[20] A. Tripathi and G. Narayanan, "Evaluation and minimization of low-order harmonic torque in low-switching-frequency inverter-fed induction motor drives," *IEEE Trans. Ind. Appl.*, vol. 52, no. 2, pp. 1477–1488, Mar./Apr. 2016.
[21] A. Edpuganti and A. K. Rathore, "A survey of low switching frequency modulation techniques for medium-voltage multilevel converters," *IEEE Trans. Ind. Appl.*, vol. 51, no. 5, pp. 4212–4228, Sep./Oct. 2015.
[22] G. R. Walker, "Digitally-implemented naturally sampled PWM suitable for multilevel converter control," *IEEE Trans. Power Electron.*, vol. 18, no. 6, pp. 1322–1329, Nov. 2003.
[23] D. G. Holmes and B. P. McGrath, "Opportunities for harmonic cancellation with carrier-based PWM for a two-level and multilevel cascaded inverters," *IEEE Trans. Ind. Appl.*, vol. 37, no. 2, pp. 574–582, Mar./Apr. 2001.
[24] K. Ilves, L. Harnefors, S. Norrga, and H. P. Nee, "Analysis and operation of modular multilevel converters with phase-shifted carrier PWM," *IEEE Trans. Power Electron.*, vol. 30, no. 1, pp. 268–283, Jan. 2015.
[25] D. Grahame Holmes and T. A. Lipo, *Pulse Width Modulation for Power Converters: Principles and Practice*. Hoboken, NJ, USA: Wiley, 2003.

Saroj Kumar Sahoo (SM'16) received the B.E. degree in electrical engineering from the Biju Pattnaik University of Technology, Rourkela, India, in 2008, and the M.Tech. degree in machine drives and power electronics in 2011 from the Indian Institute of Technology, Kharagpur, India, where he is currently working toward the Ph.D. degree in the Electrical Engineering Department.

His research interests include control of traction drives, low switching frequency PWM techniques, multilevel converters, etc.

Tanmoy Bhattacharya (M'11) received the B.E. degree in electrical and electronics engineering from the National Institute of Technology, Tiruchirapalli, India, in 2002, and the M.Sc. (Eng.) and Ph.D. degrees in power electronics from the Indian Institute of Science (IISc), Bangalore, in 2005 and 2009, respectively.

He also worked as a Research Fellow with the National University of Singapore, Singapore. He is currently working as an Assistant Professor in the Electrical Engineering Department, Indian Institute of Technology, Kharagpur, India. His research interests include hybrid electric vehicles, traction drives, wind, solar hybrid systems, renewable powered microgrids, etc.